FAT1 Promotes EGFR-TKI Resistance in Non-Small Cell Lung Cancer Cells by Inducing Mitophagy

Chen Ding[1, 2#], Hua Huang[1#], Zexia Zhao[1#], Wenhao Zhao[1], Xuanguang Li[1], Hongbing Zhang[1], Minghui Liu[1], Chen Chen[3], Yongwen Li[3], Hongyu Liu[3*], Jun Chen[1,2, 3*]

1. Department of Lung Cancer Surgery, Center of Thoracic Surgery, Tianjin Medical University General Hospital, Tianjin 300052, People's Republic of China

2. Department of Thoracic Surgery, First Affiliated Hospital, School of Medicine, Shihezi University, Shihezi 832003, China.

3. Tianjin Key Laboratory of Lung Cancer Metastasis and Tumor Microenvironment, Tianjin Lung Cancer Institute, Tianjin Medical University General Hospital, Tianjin 300052, People's Republic of China

[#]These authors contributed equally in this work.

*Correspondence: junchen@tmu.edu.cn

Hongyu Liu: liuhongyu123@hotmail.com

Supplementary Methods.

Flow Cytometry Gating Strategies

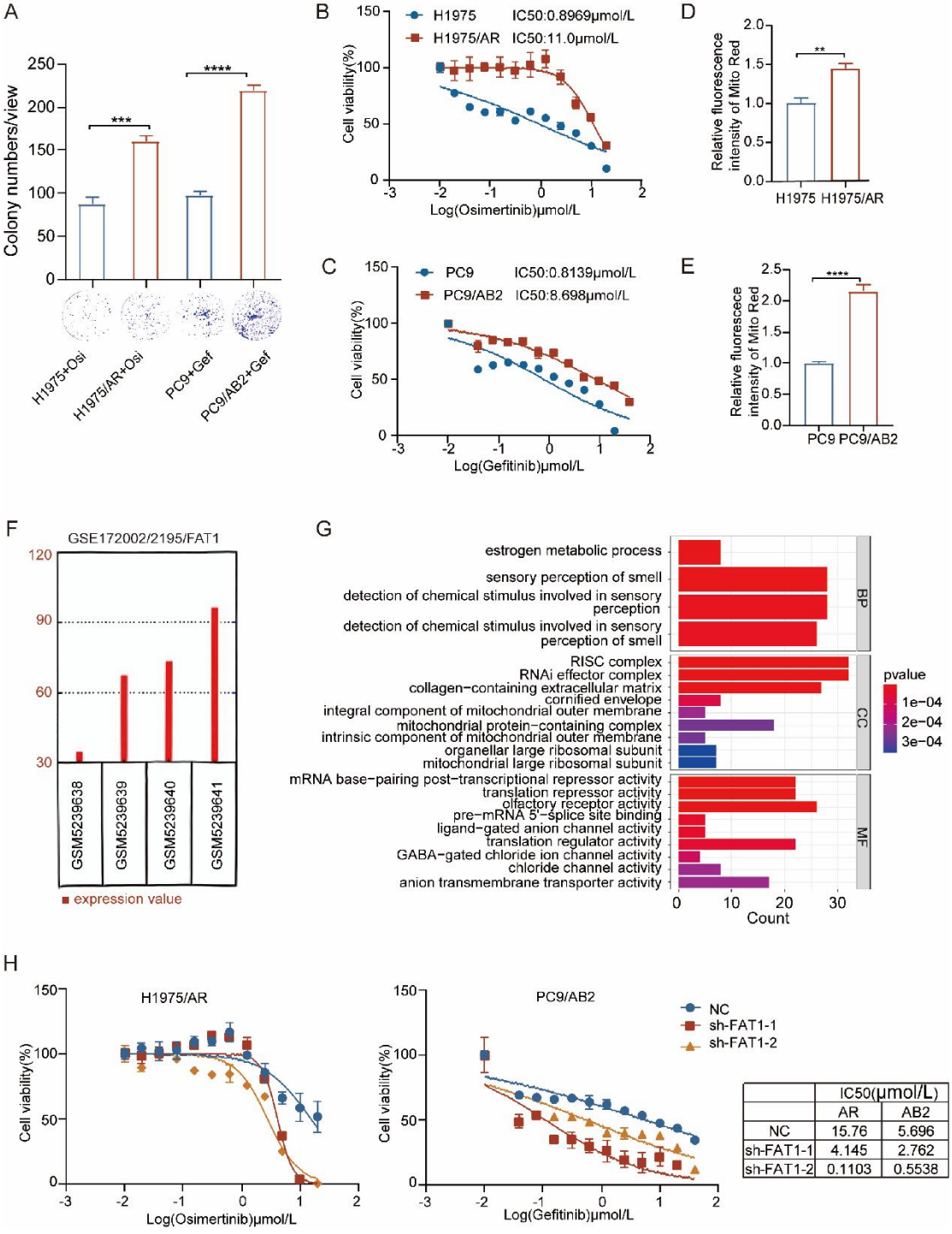
JC-1 gating strategy

Cellular events were first gated on an FSC-H versus SSC-H plot to identify the main cell population and exclude cellular debris. Singlet cells were subsequently selected using FSC-A versus FSC-H gating to exclude doublets and cell aggregates. JC-1 fluorescence was then analyzed within the gated singlet population using the FITC and PE channels, corresponding predominantly to JC-1 monomers and aggregates, respectively. Mitochondrial membrane potential was evaluated according to the red-to-green JC-1 fluorescence ratio, with a reduced red/green ratio indicating mitochondrial depolarization. The same gating strategy was applied consistently to all experimental groups.

Total ROS gating strategy

For flow cytometric analysis, cellular events were first gated on an FSC-A versus SSC-A plot to identify the main cell population and exclude cellular debris. FITC-A fluorescence was subsequently analyzed within the gated population to assess intracellular ROS levels. The same gating strategy was applied consistently to all experimental groups.

Supplementary Figures

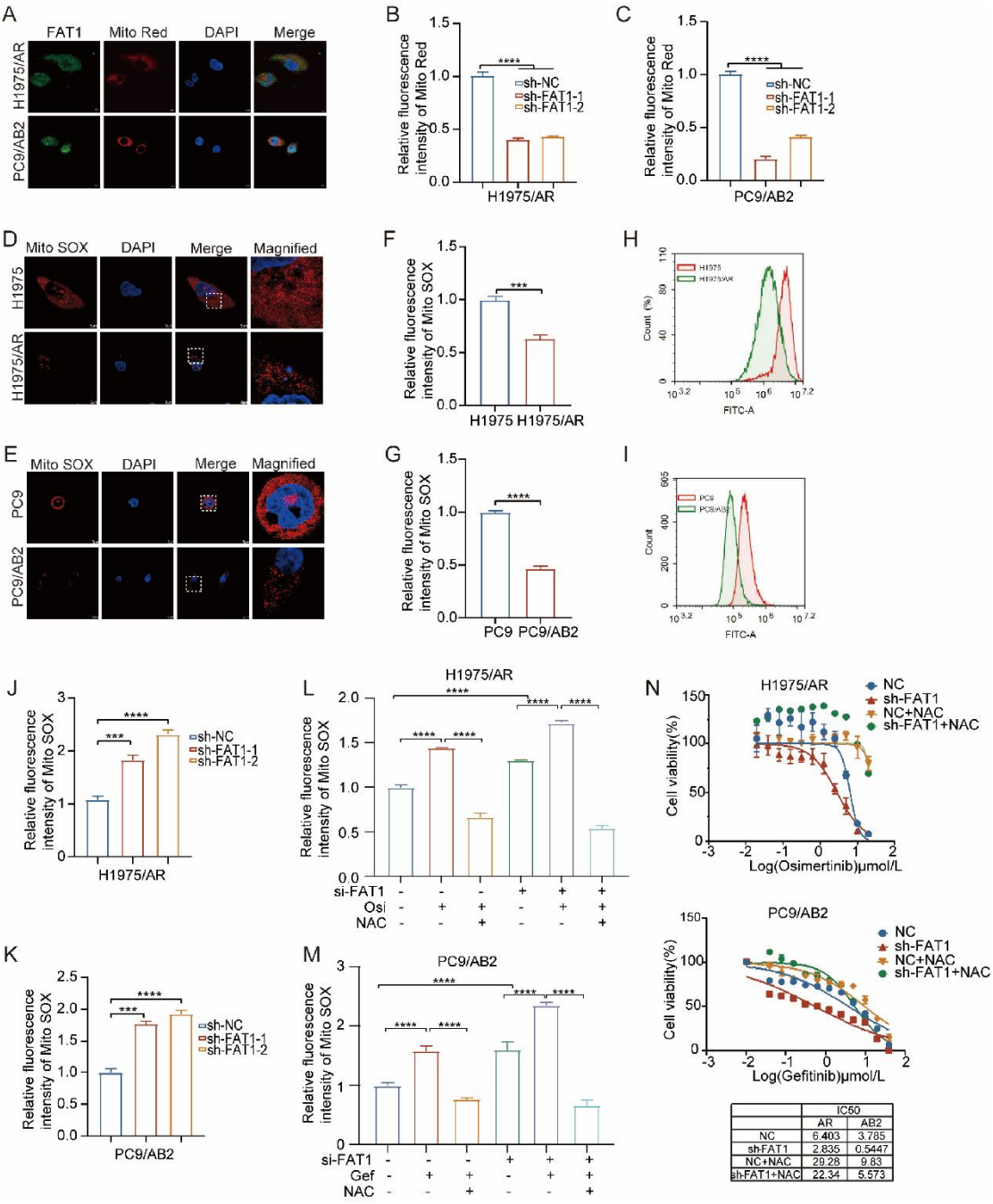


	IC50(μmol/L)	
	AR	AB2
NC	15.76	5.696
sh-FAT1-1	4.145	2.762
sh-FAT1-2	0.1103	0.5538

Figure S1. Establishment and mitochondrial characterization of EGFR-TKI-resistant NSCLC cell models

(A) Colony formation assays showing reduced EGFR-TKI sensitivity in resistant cells compared with their parental counterparts. (B, C) CCK-8 assay showing higher IC50 values in resistant cells than in parental cells. (D, E) Quantification of Mito Tracker Red fluorescence intensity in parental and resistant cells. (F) GEO database analysis

showing increased FAT1 expression in resistant versus sensitive cell lines. (G) Functional enrichment analysis of FAT1-associated biological processes and cellular components. (H) CCK-8 assay showing increased EGFR-TKI sensitivity after FAT1 knockdown in resistant NSCLC cells. (mean ± SD, n=3, **p<0.01, ***p<0.001, ****p<0.0001).



	IC50	
	AR	AB2
NC	6.403	3.785
sh-FAT1	2.835	0.5447
NC+NAC	29.28	9.83
sh-FAT1+NAC	22.34	5.573

Figure S2. FAT1 regulates mitochondrial integrity and ROS homeostasis in resistant NSCLC cells. (A) Colocalization of FAT1 with mitochondria labeled by MitoTracker Red. Scale bar, 5μm. (B, C) Quantification of MitoTracker Red fluorescence intensity after FAT1 knockdown. The data are presented as relative mean fluorescence intensity. (D-G) Mitochondrial ROS levels in TKI-sensitive and resistant NSCLC cells. Scale bar, 5μm. (H, I) Total intracellular ROS levels in TKI-sensitive and resistant NSCLC cells. (J, K) FAT1 knockdown leads to increased mROS generation, as measured by fluorescence intensity. The data are presented as relative mean

fluorescence intensity. (L, M) EGFR-TKIs induced mitochondrial ROS accumulation in FAT1-knockdown cells is reversed by NAC. The data are presented as relative mean fluorescence intensity. (N) CCK-8 assay showing the effect of NAC on drug sensitivity after FAT1 knockdown.

(mean±SD, n=3, ***p<0.001, ****p<0.0001).

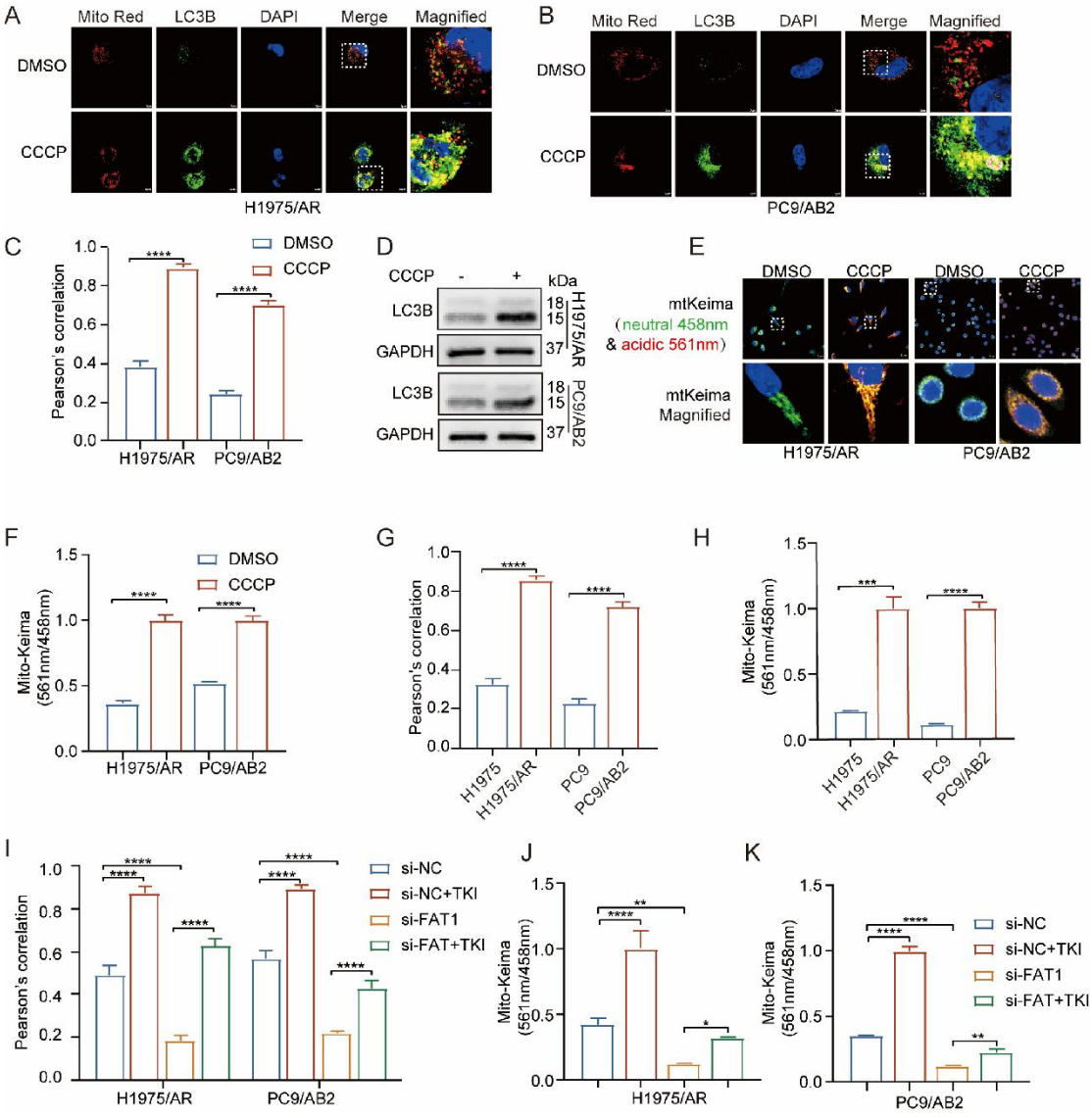


Figure S3. Validation of mitophagy assays and additional analyses of mitophagy in sensitive and resistant NSCLC cells. (A-C) Immunofluorescence analysis showing increased LC3B-Mito Tracker Red colocalization after CCCP treatment, indicating recruitment of autophagic machinery to mitochondria. Scale bar, 5μm. (D) Western blot analysis showing increased LC3B protein levels after CCCP treatment. (E, F) Mito-Keima analysis showing increased mitochondrial delivery to acidic lysosomal compartments after CCCP treatment, confirming mitophagy activation. Scale bar: 5μm. (G) Quantification of LC3B-Mito Tracker Red colocalization in sensitive and resistant NSCLC cells. (H) Quantification of mito-Keima signal in sensitive and resistant NSCLC cells. (I) Quantification of LC3B-Mito Tracker Red colocalization in resistant cells under FAT1 knockdown and EGFR-TKI treatment. (J, K) Quantification of mito-Keima signal in resistant H1975/AR and PC9/AB2 cells under FAT1 knockdown and

EGFR-TKI treatment. (mean ± SD, n=3, *p<0.05, **p<0.01, ***p<0.001, ****p<0.0001).

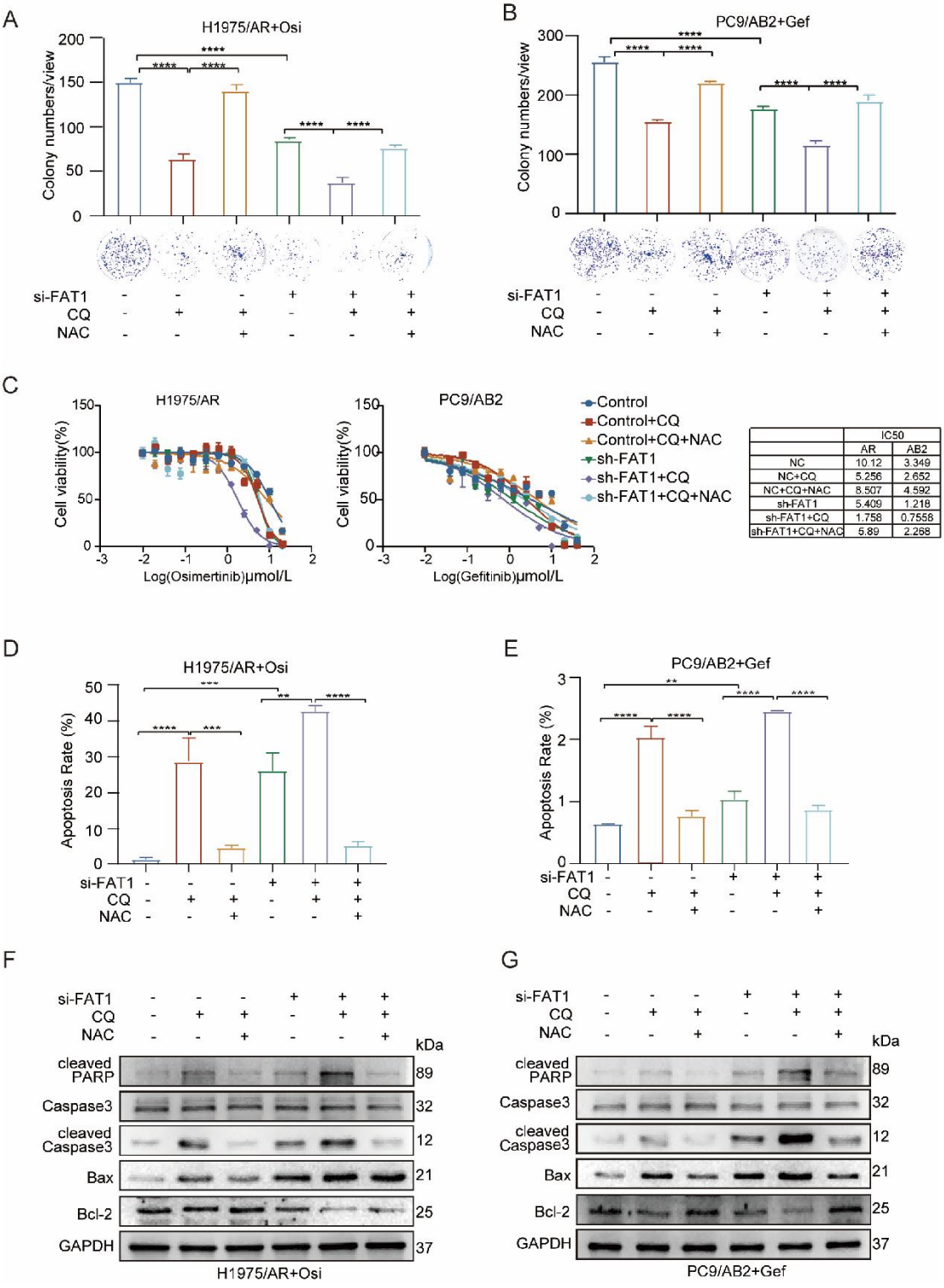


Figure S4. Mitophagy-mediated control of mROS contributes to FAT1-dependent EGFR-TKI resistance. (A, B) Colony formation assays showing that CQ reduces clonogenic survival of EGFR-TKI-resistant NSCLC cells and that NAC partially reverses this effect. (C) CCK-8 assays showing the same trend under CQ and NAC treatment. (D, E) Flow cytometric analysis of apoptosis showing that CQ increases apoptosis in resistant cells and that NAC attenuates this effect. (F, G) Western blot

analysis of apoptosis-related proteins, including caspase3, cleaved caspase-3, cleaved PARP, BAX, and BCL-2, under CQ and NAC treatment. (mean ± SD, n=3, **p<0.01, ***p<0.001, ****p<0.0001).

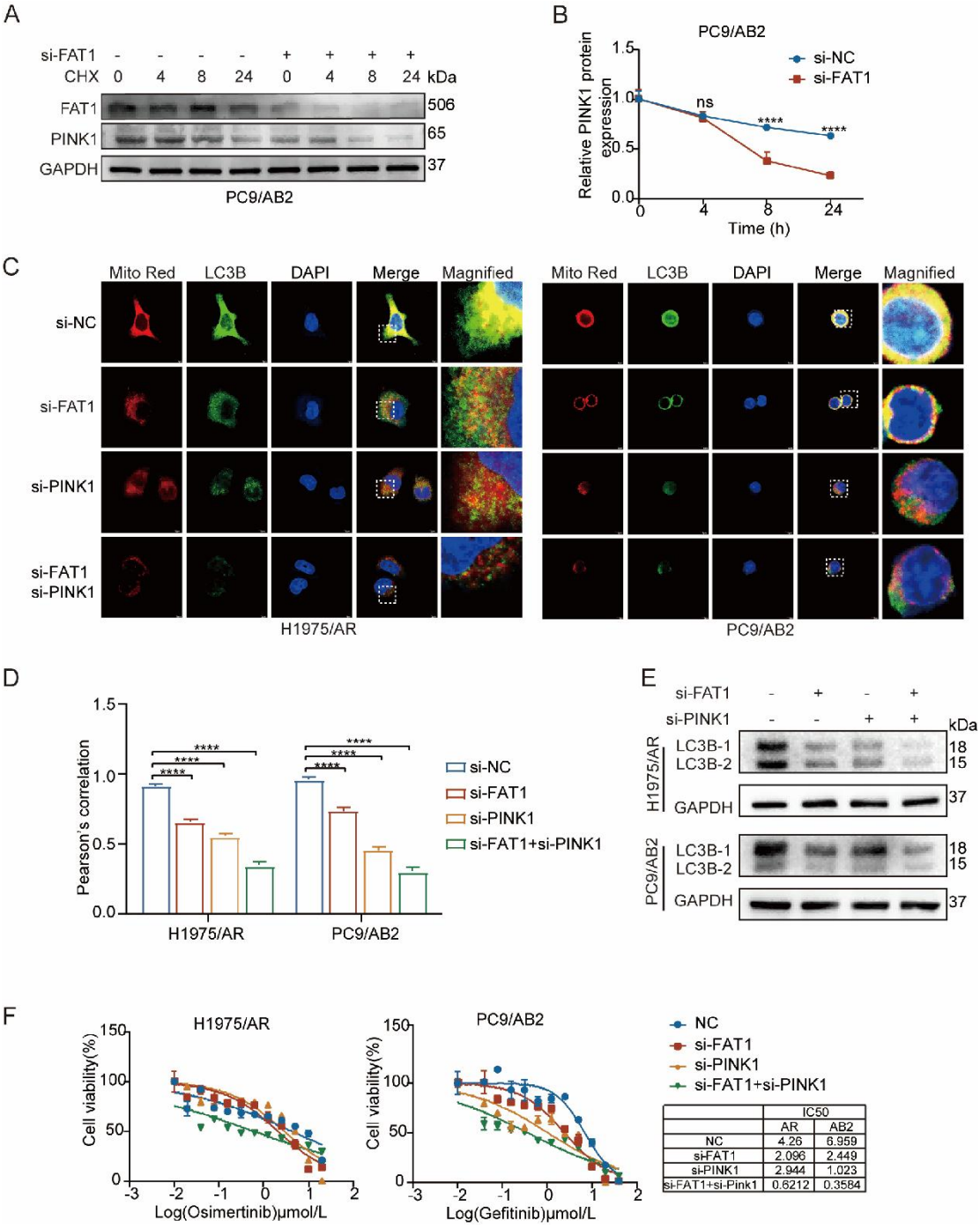


Figure S5. FAT1/PINK1 co-regulate mitophagy and drug sensitivity. (A, B) Cycloheximide (CHX) reveals a shorter PINK1 half-life after FAT1 knockdown. (C, D) Immunofluorescence analysis showing reduced LC3B – Mito Tracker Red colocalization after FAT1 or PINK1 knockdown, with a stronger effect after combined knockdown. Scale bar, 5μm. (E) Western blot analysis of autophagy-related markers under the indicated conditions. (F) CCK-8 assay showing increased EGFR-TKI sensitivity after FAT1 or PINK1 knockdown. (mean ± SD, n=3, $^{ns}p>0.05$,

102 ****p<0.0001).

103

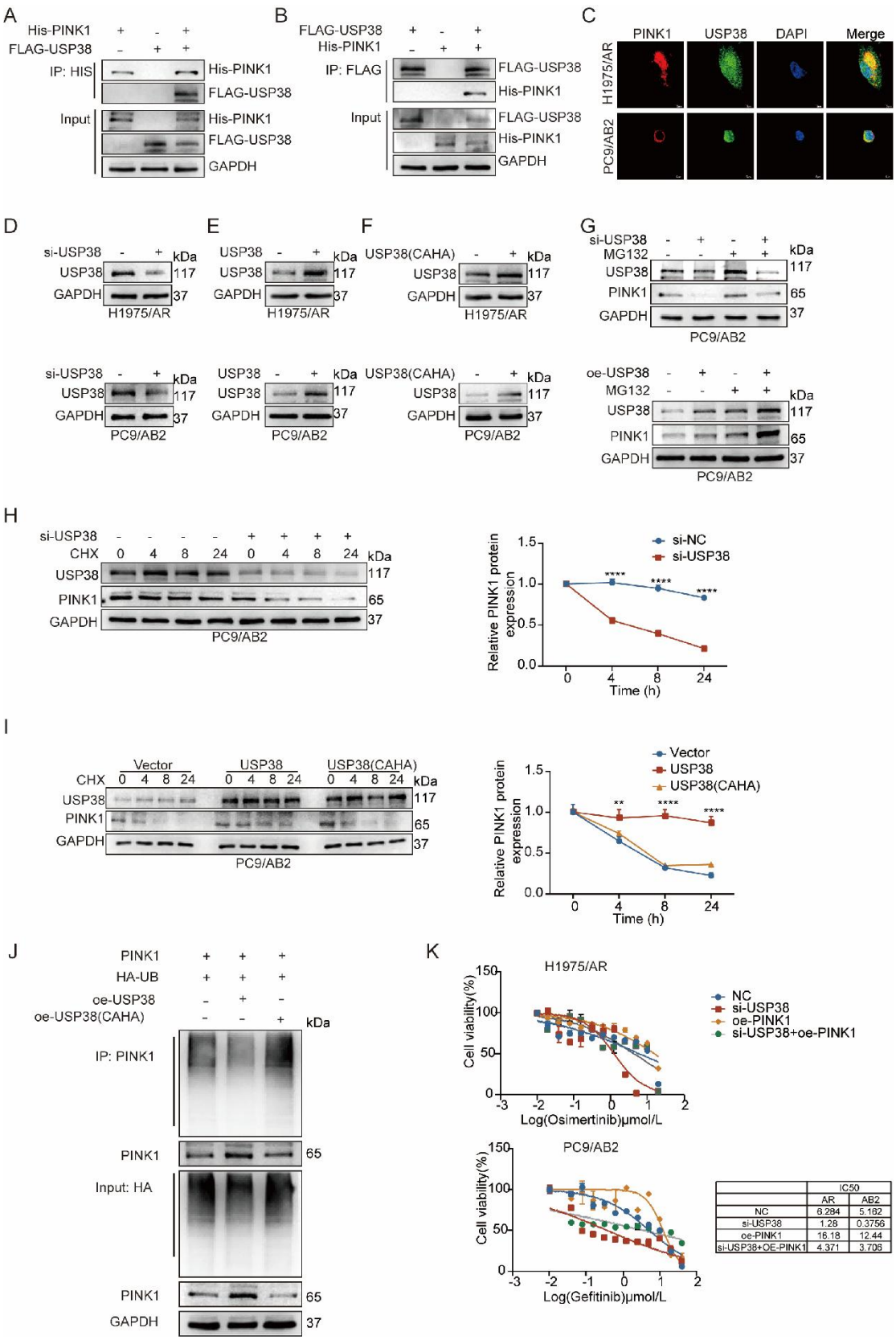


Figure S6. USP38 regulates PINK1 stability and drug resistance. (A, B) Exogenous overexpression confirms the interaction between PINK1 and USP38. (C) Colocalization of USP38 and PINK1. Scale bar, 5μm. (D–F) Validation of USP38

knockdown and overexpression efficiency. (G) MG-132 treatment increases PINK1 expression. (H, I) USP38 stabilizes the half-life of PINK1 protein. (J) USP38 overexpression decreases PINK1 ubiquitination. (K) CCK-8 assay showing that USP38 knockdown enhances EGFR-TKI sensitivity and that PINK1 overexpression reverses this effect. (mean±SD, n=3, **p<0.01, ****p<0.0001).

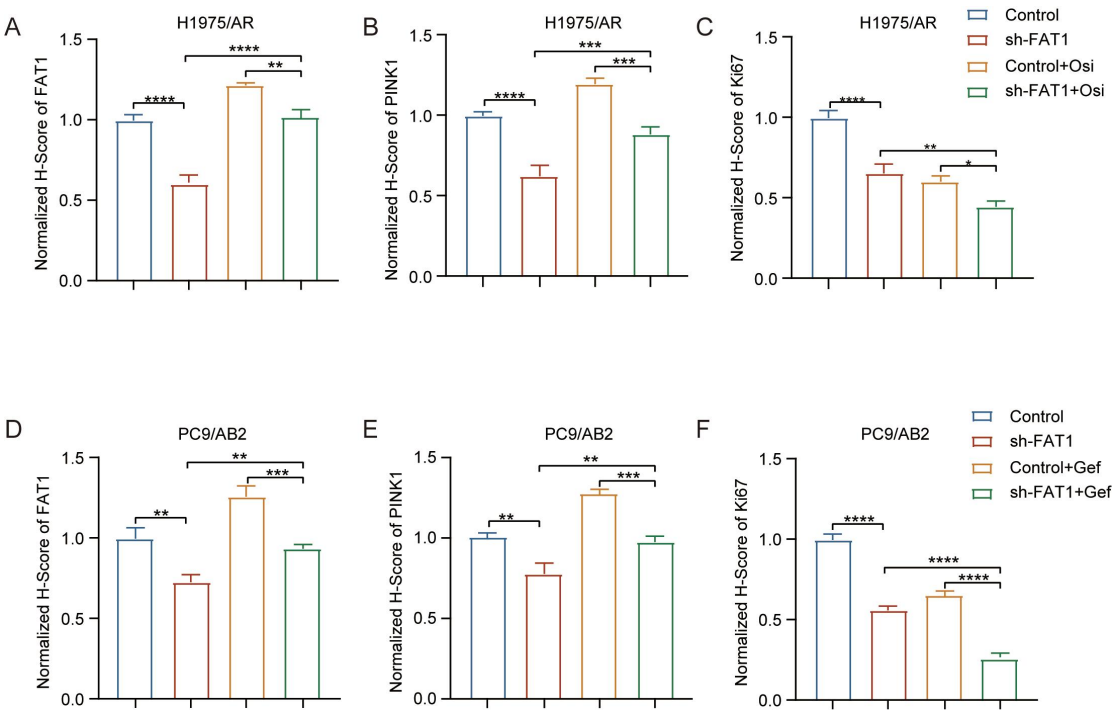


Figure S7. (A-C) Quantitative analysis of FAT1, PINK1 and Ki67 expression in H1975/AR xenograft tumors. (D-F) Quantitative analysis of FAT1, PINK1 and Ki67 expression in PC9/AB2 xenograft tumors. (mean ± SD, n=5, *p<0.05, **p<0.01, ***p<0.001, ****p<0.0001).

Table S1. siRNA sequences for gene knockdown

GENE	Sequence
FAT1	5′-GCACCACAAUUUCGAGCAATT-3′
PINK1	5′-CCTAACCGTCTCCGCTTCTTC-3′
USP38	5′-GGGTAATTGCACTCCTGAATT-3′

Table S2. Antibodies used in Western blot analysis, immunofluorescence, and immunoprecipitation:

Antibody	WB	IF	IHC	Supplier	Catalogue
GAPDH	1:10000	-	-	Proteintech	60004-1-Ig
FAT1	1:1000	1:200	1:200	Abcam	ab190242
Caspase3	1:1000	-	-	Proteintech	19677-1-AP
Cleaved-Caspase3	1:1000	-	-	Proteintech	68773-1-Ig
Cleaved-PARP	1:1000			CST	D64E10
Bax	1:1000	-	-	Proteintech	50599-1-Ig
Bcl-2	1:1000	-	-	Proteintech	12789-1-AP
LC3B	1:1000	1:200	1:200	Proteintech	18725-1-AP
COX IV	1:1000	-	-	Proteintech	11242-1-AP
P62	1:1000	-	-	Abcam	ab91526
Beclin-1	1:1000	-	-	CST	D40C5
PINK1	1:800	1:200	1:200	Santa Cruz	sc-518052
anti-ubiquitin	1:1000	-	-	CST	E6K4Y
USP38	1:1000	-	-	Proteintech	17767-1-AP
Anti-rabbit	1:5000	-	-	Abclonal	AS014
Anti-mouse	1:5000	-	-	Abclonal	AS003
AF488 anti-rabbit	-	1:200	-	ZSGB-BIO	ZF-0511
AF594 anti-mouse	-	1:200	-	ZSGB-BIO	ZF-0513
AF488 anti-mouse	-	1:200	-	ZSGB-BIO	ZF-0512

Supplier location: CST: Cell Signaling Technology (Danvers, MA, USA). Proteintech (Wuhan, China). ABclonal Biotechnology (Wuhan, China). Santa Cruz Biotechnology(Santa Cruz, CA, USA). Abcam (Cambridge, UK) , ZSGB-BIO: Zhongshan Golden Bridge Biotechnology (Beijing, China)

128 **Table S3. Primers sequences (5′-3′):**

GAPDH	Forward	GGAGCGAGATCCCTCCAAAA
	Reverse	GGCTGTTGTCATACTTCTCATGG
FAT1	Forward	CATCCTGTCAAGATGGGTGTTT
	Reverse	TCCGAGAATGTACTCTTCAGCTT
USP1	Forward	GCGTTGCTTGGAATGTGAAAG
	Reverse	CCATCTCAGGGTCTTCATTTCTG
USP2	Forward	CCTAAGTCCAACCCTGAGAAC
	Reverse	ACCACAATCTGTACACGTCAG
USP3	Forward	CGTGGAGTTAAGGAATGGGAA
	Reverse	AAGGACTCTGGGCTAAATGC
USP4	Forward	CAGGGTCAGGTGCTAGTAATTG
	Reverse	CAGAGCCCAGGTTGTATATGAG
USP5	Forward	GGAAGTATGTGGATAAGCTGGAG
	Reverse	CGGTACTGGCTTGGAATACTC
USP6	Forward	ACCTTCGCTATCAAACATCCC
	Reverse	GTACATCTCACTTTCCCCTAGC
USP7	Forward	CCAGGAGAAGGAGTTTGAGAAG
	Reverse	GGCCGAGGATGAGACATATTAC
USP8	Forward	AAGGCAGGAAACAGGAAGAG
	Reverse	CTGTGATTGCTCCTTTCTCTTTG
USP10	Forward	GATCAATAAAGGGAACTGGTGC
	Reverse	AGCTGTCTATCATGGGTGTTG
USP11	Forward	GTATAACGTCCTGATGTACCGG
	Reverse	CTTTCTCATCCCCATCGTCC
USP12	Forward	TGTGATTGGGTGGAAGATGG
	Reverse	CAAAATAGTGCTCATTGACCGG
USP13	Forward	ATTCAGTGCTGTCAGACCC
	Reverse	CTTCTGCTTCCCTTCTCGTTAG
USP14	Forward	TGGCTTCAGCGCAGTATATTAC
	Reverse	TGTCCTTGTTCACCTTTCTCG
USP15	Forward	GGTCCTTGCCGCTATAATCTG
	Reverse	TTGGTCTTCAGATGCAGTGG
USP16	Forward	GATCTGAACCTCACTGTCTGG
	Reverse	TGTAATGCTGGCTTGTTTTCTG
USP18	Forward	TCATGCGATTCTCCATCAGG

	Reverse	AAAAGCTCATACTGCCCTCC
USP19	Forward	ATGTGAAGCCTGAGAACCTG
	Reverse	CTTAGCCAACTCTGAGGATAGC
USP20	Forward	ACCTTTGCCCTCACCTTG
	Reverse	TTCTCCGCAGCCAACATAG
USP22	Forward	GAGAGCAGGATGAATGGACAG
	Reverse	CGGATAAAGCTGGTGTAGTGG
USP24	Forward	CTTCTGCTCTTGATACCCACTG
	Reverse	CTGGTGCTGTTGCTTTGATG
USP25	Forward	AAGAGAAGCCAAAGAACCCC
	Reverse	TGAACCCATTGACCTGAAGTG
USP26	Forward	AGAATCTGTGAACAAGCCCC
	Reverse	TTGGAACCCAGTGCAAGTAG
USP29	Forward	AGACCTGGAAAATGGCTCTG
	Reverse	CCCTCCATCTTCATACATCACAG
USP30	Forward	ATTGGAAGATGAGCGAGACC
	Reverse	GTGATTGGATGTAGGGTGAGG
USP31	Forward	AATTCCTCTGCCCCACAC
	Reverse	TTTCCATAGACACTGCTTCCC
USP32	Forward	ACCTTCGCTATCAAACATCCC
	Reverse	CTCATTTTCCCCTAGCTCTTCC
USP33	Forward	GGATAGGAAATTAGGAACTCAGCC
	Reverse	TCAAATACGGCAACCAGAGG
USP34	Forward	GTCTACACGCCCTTATCTTCAG
	Reverse	CCTTGAGGACATCTATACAGGC
USP36	Forward	TCTCAAATGCCCAAGGAGTG
	Reverse	CTCTCCATTCCAAGACACAGG
USP37	Forward	GAAGAGAATAGGACATCAGGGC
	Reverse	GAGGGAGTCTGGCTTGAAAC
USP38	Forward	TCTCCCAGGTGACAAAAGTG
	Reverse	GCTTGCCAATGCTACAGAAG
USP39	Forward	GCTTCCCCATCCTGATCTG
	Reverse	GCTCCTTCTCGTCCTTGTAG
USP43	Forward	GTTCCTGACTCTCCCATCTTC
	Reverse	TCTTGAATGGTCCCTGCTTG
USP44	Forward	GTCTGGTTACTGAAATGTTGGC

	Reverse	TGTTTCTGGGCTTCTGTGAG
USP46	Forward	TTGTAAAGATGGCGGTGAGG
	Reverse	TGATTGGAAACTGCTCTGGAC
USP47	Forward	CAGGTTTATAGGTCCGCTTCC
	Reverse	TGCTTGGTTTACTAGTCCCAC
USP48	Forward	TCTCAGACACGTAAACCCAAG
	Reverse	GAATTATCCCGATCTACCAGCTC
USP49	Forward	ATCTACGCTTGTGACCAGTG
	Reverse	GAATCTTTTAAGGTGCAGCCG
USP50	Forward	CTTCTCACTCCCCATTCCATC
	Reverse	GGTTTCACAAAAGGAGCAGTG
USP51	Forward	AGCCTGCCATAGTGTTTCTAC
	Reverse	TGGGTTCTGGGAATCGAATG
USP52	Forward	TGTTTCCGTCTCCCACTTTG
	Reverse	GCTCTGGATCTGCCGAATATC
USP54	Forward	TCATATCCCAAAGTCGCACAG
	Reverse	ACCTCTTCCTGCAATTCATCC